

# Factors controlling dissolved $^{137}\text{Cs}$ activities in Matsukawa-ura lagoon, a semi-closed estuary, after the Fukushima accident

Takuya Niida<sup>1,2</sup>, Hyoe Takata<sup>3</sup>, Sho watanabe<sup>4</sup>, Shinya Namura<sup>2</sup>, Toshihiro Wada<sup>3</sup>

<sup>1</sup> Graduate School of Symbiotic Systems Science and Technology, Fukushima University, 1 Kanayagawa, Fukushima City, Fukushima 960-1296, Japan

<sup>2</sup> Laboratory for Instrumentation and Analysis, Environmental Engineering Division, KANSO TECHNOS CO., LTD, 3-1-1, Higashikuraji, Katano City, Osaka 576-0061, Japan

<sup>3</sup> Institute of Environmental Radioactivity, Fukushima University, 1 Kanayagawa, Fukushima City, Fukushima 960-1296, Japan

<sup>4</sup> Fukushima Prefectural Research Institute of Fisheries Resources, 1-1-14 Koyo, Soma City, Fukushima 970-0005, Japan

*Correspondence to:* Takuya Niida (niida\_takuya@kanso.co.jp)

**Abstract.** The spatial and seasonal dynamics of  $^{137}\text{Cs}$  were investigated from 2021 to 2023 in Matsukawa-ura lagoon, a semi-closed estuarine area approximately 40 km north of the Fukushima Daiichi Nuclear Power Plant (FDNPP), Japan. Weighted mean dissolved  $^{137}\text{Cs}$  concentrations in the lagoon waters ranged from 5.3 to 19 Bq m<sup>-3</sup>, 2.4–8.6 times higher than those in the surrounding coastal seawater and inflowing river waters. Furthermore, dissolved  $^{137}\text{Cs}$  concentrations in the lagoon were higher in summer than in winter and strongly correlated with water temperature. Mass balance calculations imply that continuous  $^{137}\text{Cs}$  input from the river is unlikely to contribute to the spatiotemporal variability of dissolved  $^{137}\text{Cs}$  concentrations and  $^{137}\text{Cs}$ , deposited during the early stages of the FDNPP accident, exposed to seawater flowing into the lagoon and gradually dissolved from bottom sediments maintains high dissolved  $^{137}\text{Cs}$  concentration in the lagoon. These results indicate that warmer waters during the summer accelerate the dissolution of  $^{137}\text{Cs}$  from bottom sediments and suggest that suggest the importance of the dynamics of  $^{137}\text{Cs}$  through bottom sediments and pore waters in the coastal areas of Fukushima Prefecture.

## 1 Introduction

The Fukushima Dai-ichi Nuclear Power Plant (FDNPP) accident on 11 March 2011 released important amounts of radioactive Cs ( $^{134}\text{Cs}$  and  $^{137}\text{Cs}$ ) into the surrounding areas and the North Pacific. It is estimated that a total of 15–20 PBq of  $^{137}\text{Cs}$  was released into the atmosphere between 12 March and 30 April 2011, with 10%–40% (2–6 PBq) estimated to have been deposited in eastern Japan (Aoyama et al., 2016). Currently, the dissolved  $^{137}\text{Cs}$  activity concentration in seawater more than 30 km offshore Fukushima has returned to pre-accident levels (Kusakabe and Takata, 2020), whereas that in coastal waters of Fukushima Prefecture remains above pre-accident levels (Suzuki et al, 2022). Potential sources of dissolved  $^{137}\text{Cs}$  in Fukushima coastal waters include direct inflow from the FDNPP, leaching from seabed sediments, and inflow from rivers. The completion of impermeable seaside wall in 2016 may have recently limited direct inflow from the FDNPP (Machida et al., 2019). Otosaka et al. (2020) estimated the dissolved  $^{137}\text{Cs}$  concentrations in pore waters within bottom sediments to be 10–

40 times higher than that in the overlying water (seawater approximately 60 cm above the seafloor), suggesting that the leaching of radioactive Cs from sediments to pore water is a  $^{137}\text{Cs}$  source in coastal areas.

35 Extensive studies of the riverine transport of  $^{137}\text{Cs}$  from land to estuaries revealed that most of the  $^{137}\text{Cs}$  transported from land to ocean is in the particulate phase (e.g., Nagao et al., 2013; Yamashiki et al., 2014; Niida et al., 2022). Although the proportion of dissolved  $^{137}\text{Cs}$  supplied by rivers is extremely small, dissolved  $^{137}\text{Cs}$  concentrations in the marine environment tend to be higher at near-shore sites (e.g., river mouths) than in offshore waters (Takata et al., 2020a). Accordingly, the supply from rivers to the marine environment is considered to increase dissolved  $^{137}\text{Cs}$  concentrations. This supply is mainly regulated by water temperature and the competition between particulate-bound  $^{137}\text{Cs}$  and ions in seawater, as described below.

40 Recent studies in rivers suggested that the distribution coefficient between particulate-bound  $^{137}\text{Cs}$  and dissolved  $^{137}\text{Cs}$  decreases with increasing water temperature, making it easier for  $^{137}\text{Cs}$  to be released from suspended particles in rivers during the warmer summer season (Igarashi et al., 2022; Tsuji et al., 2023). Furthermore, Machida et al. (2019) estimated the  $^{137}\text{Cs}$  outflow from the harbor of the FDNPP and reported higher levels in summer than in winter, indicating that the dissolved  $^{137}\text{Cs}$  concentrations in the harbor may be related to water temperature.

45 Experiments reproducing the interaction between dissolved and particulate  $^{137}\text{Cs}$  due to the flow of particulate-bound  $^{137}\text{Cs}$  from rivers into the sea show that the distribution coefficient ( $K_d$ ) between particulate-bound  $^{137}\text{Cs}$  and dissolved  $^{137}\text{Cs}$  decreases along a salinity gradient (Li et al., 1984; Turner, 1996). These results suggest that  $^{137}\text{Cs}^+$  can be desorbed from the particles due to competition with ions such as  $\text{K}^+$  and  $\text{NH}_4^+$  (Takata et al., 2020b, 2021).

50 The relationships between water temperature and dissolved  $^{137}\text{Cs}$  concentrations in river water and between salinity and dissolved  $^{137}\text{Cs}$  concentrations in seawater are often discussed (Takata et al., 2022; Tsuji et al., 2023), but those in estuarine areas have not been sufficiently addressed. One of the reasons for this is that the dissolved  $^{137}\text{Cs}$  transported from land and leached from sediments is immediately diluted and dispersed into large amounts of seawater, making quantitative assessments challenging.

This study focuses on Matsukawa-ura lagoon (Soma City, Fukushima Prefecture) and its inflowing rivers to discuss the supply of  $^{137}\text{Cs}$  to the lagoon and the spatial and seasonal dynamics of  $^{137}\text{Cs}$  within the lagoon. Matsukawa-ura lagoon is a semi-closed estuarine area approximately 40 km north of the FDNPP, providing an ideal area for estimating the flux of  $^{137}\text{Cs}$  transported from rivers and desorbed from sediments. Additionally, the lagoon is only connected to the Pacific Ocean through a 100-m-wide mouth at its northmost point, facilitating the quantification of the mass balance of  $^{137}\text{Cs}$  within the lagoon. Kambayashi et al. (2021) investigated the distribution of  $^{137}\text{Cs}$  in Matsukawa-ura lagoon and the rivers flowing into the lagoon from 2014-2016 and calculated mass balance of  $^{137}\text{Cs}$ , suggested that  $^{137}\text{Cs}$  supplied from bottom sediments in the lagoon contribute greatly to the distribution of  $^{137}\text{Cs}$  in the lagoon, with the flux supplied from bottom sediments being highest in summer. The aim of this study was to investigate the distribution of  $^{137}\text{Cs}$  inputs, in turn allowing us to evaluate the contribution of  $^{137}\text{Cs}$  supplied by rivers to estuarine areas, the relationships with salinity and water temperature, and the contribution and seasonality of  $^{137}\text{Cs}$  dissolved from bottom sediments. Our results improve our understanding of radioactive contamination in aquatic habitats.

## 2 Material and Methods

### 2.1 Study Area and Sampling Stations

70 Matsukawa-ura lagoon is a semi-closed estuarine area with an area of 6.48 km<sup>2</sup> with fluctuating salinity and water temperature conditions (Wada et al., 2011; Noda et al., 2021). The mean water temperature in the lagoon during 1991–2021 was 15.1 °C, with a maximum of 27.1 °C and a minimum of 5.6 °C (Fukushima Prefecture). Four rivers flow into Matsukawa-ura lagoon: Koizumi River (catchment area 17.8 km<sup>2</sup>), Uda River (100.6 km<sup>2</sup>), Ume River (10.7 km<sup>2</sup>), and Nikkeshi River (22.6 km<sup>2</sup>). According to the fourth aerial survey conducted by the Ministry of Education, Culture, Sports, Science and Technology, MEXT (November 2011), the mean inventory of <sup>137</sup>Cs deposited in the Koizumi, Uda, Ume, and Nikkeshi  
75 catchments were 70, 205, 70, and 93 kBq m<sup>-2</sup> respectively, with relatively higher concentrations observed in the forested areas of the upstream Uda catchment. The mean concentration of <sup>137</sup>Cs across the entire Matsukawa-ura catchment was 163 kBq m<sup>-2</sup> (Figure 1a). Due to the impermeable bedrock in the midstream to upstream areas of the lagoon's watershed, it is considered that precipitation hardly infiltrates the underground, instead directly flowing into the rivers and delivering 52.1% of the total precipitation runoff to the lagoon through the rivers (Kamo et al., 2014). Additionally, Arita et al. (2014) estimated the total  
80 accumulation of <sup>137</sup>Cs in surface sediments (0–20 cm depth) within the lagoon to be 220 GBq as of November 2013.

In this study, we conducted 11 samplings from June 2021 to February 2023 at 13 sites including downstream sites in the four rivers, sites at the mouths of three rivers (Koizumi, Uda, and Ume Rivers), five sites within the lagoon (from the southeast to near the lagoon mouth in the north), and a site 800 m offshore along the outer coast of the lagoon (Figure 1b). Detailed sampling locations and dates are provided in Tables S1. Table S1 presents estimated flow rates for each river on each sampling  
85 date, calculated based on the Voronoi diagram determined by the locations of Japan Meteorological Agency observation stations and assuming that 52.1% of precipitation in the 30 days prior to each sampling date flows into the rivers and 3.9 % flow into the lagoon as submarine groundwater discharge, SGD. (Kamo et al., 2014).

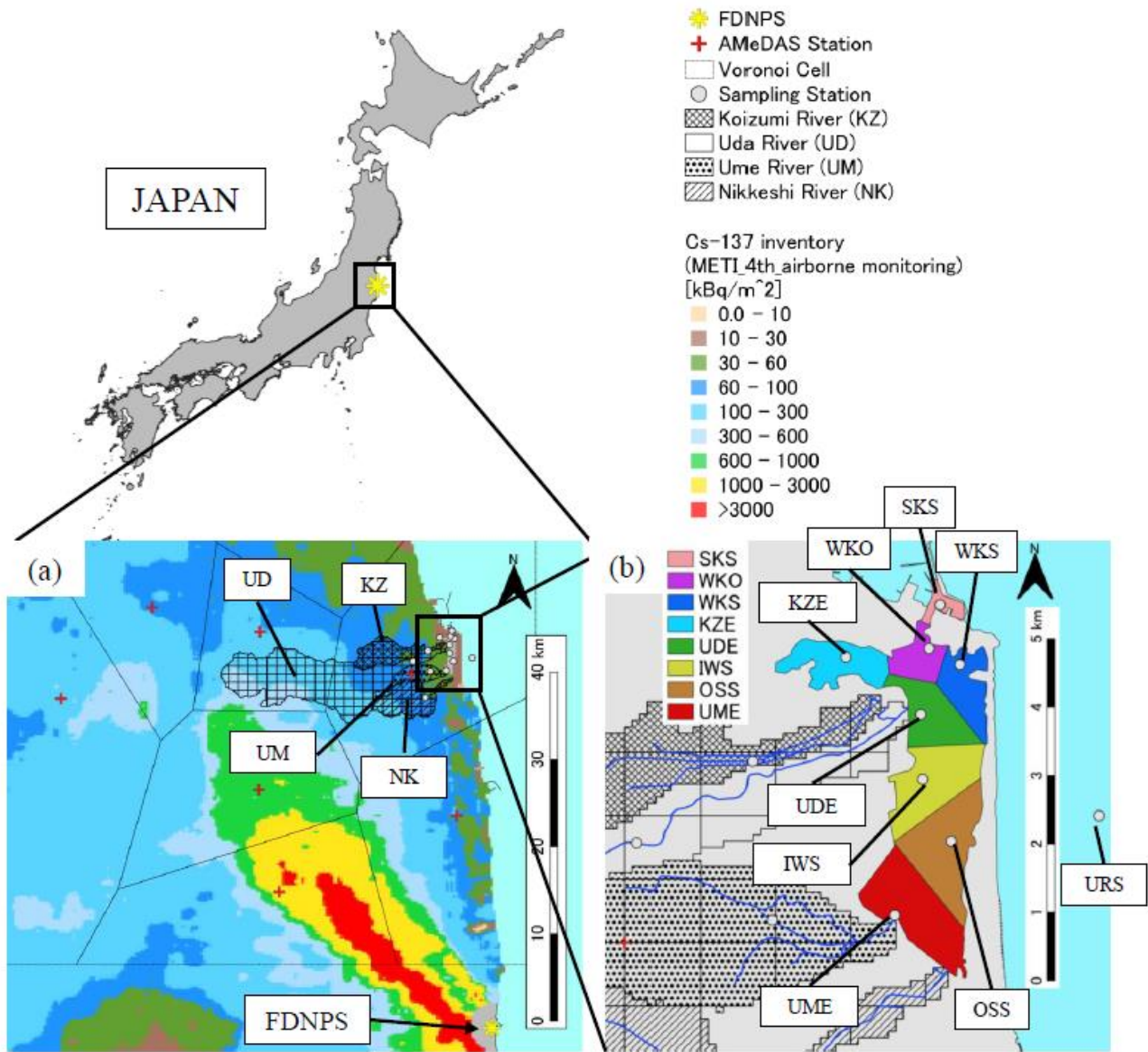


Figure 1: Spatial distribution of the  $^{137}\text{Cs}$  inventory in the study catchment (a) and sampling stations of Matsukawaura lagoon (b). The spatial distribution of the  $^{137}\text{Cs}$  inventory is based on the fourth airborne survey by MEXT (2011). The Voronoi cells were created based on the coordination of Japan Meteorological Agency weather stations (a) and sampling stations (b).

## 2.2 Sample Processing and Analysis

At each sampling site, 30–40 L of river water or surface seawater were collected using 10 L polyethylene buckets. The collected water samples were transferred to 20 L polyethylene containers and brought to the laboratory. A portion of each sample was used to measure water temperature and electrical conductivity, from which salinity was calculated. On each sampling day, the water temperature in the lagoon was measured by using a chlorophyll turbidity sensor (ACLW2-CAD, JFE Advantech Co., Ltd, Hyogo, Japan) at the station WKO, where locate at mouth of the lagoon, at 10:00 JST. Additionally, we measured the water depth at the station WKO from December 29, 2021. Water samples were filtered using a 0.45  $\mu\text{m}$  membrane filter (047-MFPES045, AS ONE Corporation, Osaka, Japan), and approximately 20 L of the filtrate were stored for dissolved  $^{137}\text{Cs}$  analysis. Additionally, 1–2 L of each sample were filtered through pre-weighed 0.4  $\mu\text{m}$  polycarbonate filters (16040004, ADVANTEC, Tokyo, Japan) to measure the suspended particle concentration, SPc ( $\text{g m}^{-3}$ ). The filters used for filtering 30–40 L of water were air-dried for about one week at 30  $^{\circ}\text{C}$ , then placed in 100 mL polyethylene containers for measurement of particle-bound  $^{137}\text{Cs}$  concentration in suspended particles,  $^{137}\text{Cs}_{\text{sp}}$  ( $\text{Bq kg}^{-1}\text{-dry}$ ), using a non-destructive gamma-ray spectrometer with a coaxial high-purity Ge detector (HPGe) (GEM40, SEIKO EG&G, Tokyo, Japan). The results were then divided by SPc to calculate particulate  $^{137}\text{Cs}$  concentration,  $^{137}\text{Cs}_{\text{par}}$  ( $\text{Bq m}^{-3}$ ). The detection limits for  $^{137}\text{Cs}_{\text{sp}}$  ranged from 4.5 to 1590  $\text{Bq kg}^{-1}\text{-dry}$  for measurement times of 80,000 s to 300,000 s, respectively. The counting efficiencies of these HPGe semiconductor detectors were calibrated using volume standard sources (MX033U8PP, The Japan Radioisotope Association, Tokyo, Japan).

To analyze dissolved  $^{137}\text{Cs}$  concentration,  $^{137}\text{Cs}_{\text{dis}}$  ( $\text{Bq m}^{-3}$ ), we followed the method reported Aoyama et al. (2013), summarized here. The filtrate stored for  $^{137}\text{Cs}_{\text{dis}}$  analysis was adjusted to a pH of approximately 1.6 with 15 M  $\text{HNO}_3$ . Then, 0.39 g of CsCl was added as a carrier and stirred for 2 h. Subsequently, Cs was coprecipitated with 6 g of ammonium phosphomolybdate (AMP, KANSO TECHNOS Co., LTD, Osaka, Japan). The  $^{137}\text{Cs}$  concentration present as an impurity in the AMP was 0.05  $\text{mBq/g-AMP}$ . The Cs-AMP precipitate was left overnight to settle, then filtered using a paper filter with a pore size of 1  $\mu\text{m}$ . After air-drying the filter for about one week at 30  $^{\circ}\text{C}$ , the precipitation was enclosed in a 10 mL Teflon container, and its weight yield was determined gravimetrically. Yields exceeded 90% for all samples. The Cs-AMP compounds enclosed in the Teflon containers were measured using a non-destructive gamma-ray spectrometer with a well-type high-purity Ge detector (GWL-90-15, SEIKO EG&G, Tokyo, Japan), and the result was reported as  $^{137}\text{Cs}_{\text{dis}}$ . The detection limit for  $^{137}\text{Cs}_{\text{dis}}$  was less than 2  $\text{Bq m}^{-3}$  for all samples. The activity concentration of  $^{137}\text{Cs}$  was decay-corrected to the sampling date.

Radiocesium partitioning between the dissolved and particulate phases was evaluated using the apparent distribution coefficient,  $K_d$  ( $\text{L kg}^{-1}$ ), (IAEA, 2004). The  $K_d$  of  $^{137}\text{Cs}$  is represented as follows:

$$K_d(\text{L kg}^{-1}) = \frac{^{137}\text{Cs}_{\text{sp}}(\text{Bq kg}^{-1})}{^{137}\text{Cs}_{\text{dis}}(\text{Bq m}^{-3})} \times 10^3, \quad (1)$$

### 2.3 Calculation of Flux of dissolved $^{137}\text{Cs}$ in the Lagoon

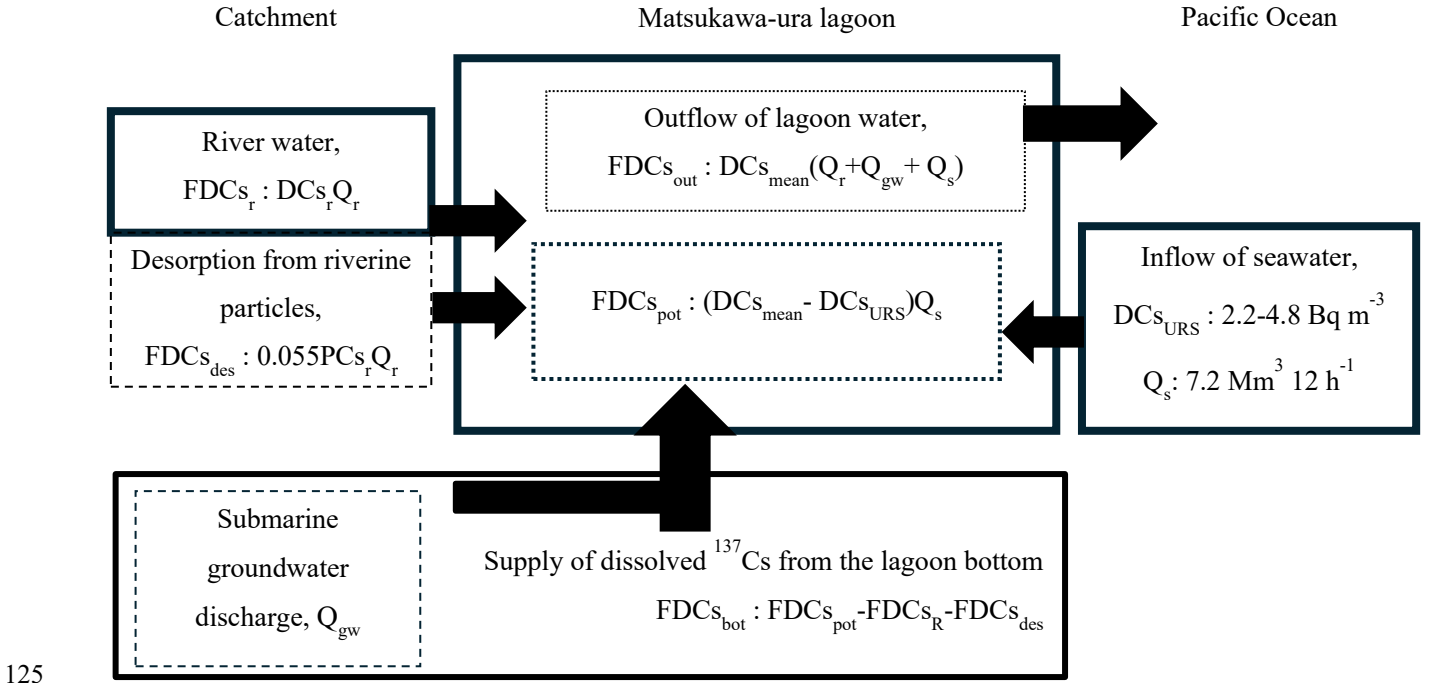


**Figure 2: Schematic illustration of the model for water and dissolved  $^{137}\text{Cs}$  in Matsukawa-ura lagoon. The volume of seawater inflow is quoted from Kamo et al. (2014). It was assumed that 5.5% of riverine particulate  $^{137}\text{Cs}$  are converted to dissolved  $^{137}\text{Cs}$  through the desorption process after flowing into the lagoon (Takata et al., 2021).**

We used mass balance calculations to evaluate the magnitudes of the internal and external sources responsible for the non-conservative mixing behavior of dissolved  $^{137}\text{Cs}$  observed in the lagoon.  $^{137}\text{Cs}$  budget in Matsukawa-ura lagoon are summarized in Figure 2.

A Voronoi partition was performed based on the sampling stations within the lagoon, and the ratio of each Voronoi cell to the area of the lagoon was used as a weighting factor when averaging the  $^{137}\text{Cs}_{\text{dis}}$  to obtain a weighted mean  $^{137}\text{Cs}_{\text{dis}}$ . The weighted mean  $^{137}\text{Cs}_{\text{dis}}$  ( $\text{Bq m}^{-3}$ ) were calculated using Eq. (2)

$$\text{DCs}_{\text{mean}} = \frac{1}{S} \times (\text{DCs}_{\text{SKS}} A_{\text{SKS}} + \text{DCs}_{\text{WKO}} A_{\text{WKO}} + \text{DCs}_{\text{WKS}} A_{\text{WKS}} + \text{DCs}_{\text{KZE}} A_{\text{KZE}} + \text{DCs}_{\text{UDE}} A_{\text{UDE}} + \text{DCs}_{\text{IWS}} A_{\text{IWS}} + \text{DCs}_{\text{OSS}} A_{\text{OSS}} + \text{DCs}_{\text{UME}} A_{\text{UME}}), \quad (2)$$

where  $\text{DCs}_{\text{mean}}$  is the weighted mean  $^{137}\text{Cs}_{\text{dis}}$  ( $\text{Bq m}^{-3}$ ),  $A$  is the area of the lagoon,  $\text{DCs}_{\text{SKS-UME}}$  ( $\text{Bq m}^{-3}$ ) are  $^{137}\text{Cs}_{\text{dis}}$  at each sampling station,  $A_{\text{SKS-UME}}$  are areas of each Voronoi cell. The potential fluxes of  $^{137}\text{Cs}_{\text{dis}}$  supplied to the lagoon were calculated by multiplying the difference in  $^{137}\text{Cs}_{\text{dis}}$  between  $\text{DCs}_{\text{mean}}$  and coastal seawater (station URS) by the volume of seawater flowing into the lagoon. The potential fluxes of dissolved  $^{137}\text{Cs}$  in the lagoon were calculated using Eq. (3).

$$\text{FDCs}_{\text{pot}} = (\text{DCs}_{\text{mean}} - \text{DCs}_{\text{URS}}) Q_s, \quad (3)$$

where  $FDC_{spot}$  is the potential fluxes of dissolved  $^{137}Cs$  ( $Bq\ 12\ h^{-1}$ ),  $DC_{SURS}$  is the  $^{137}Cs_{dis}$  at station URS ( $Bq\ m^{-3}$ ),  $Q_s$  is the volume of seawater flowing into the lagoon. The  $V_s$  value was obtained from Kamo et al. (2014) and the volume was  $7.2\ Mm^3\ 12\ h^{-1}$ .

145 The fluxes of riverine dissolved  $^{137}Cs$  flowing into the lagoon were calculated by multiplying the volume of river water discharge by the  $^{137}Cs_{dis}$  in each river. Furthermore, we assumed that 5.5% of riverine particulate  $^{137}Cs$  are converted to dissolved  $^{137}Cs$  through the desorption process after flowing into the lagoon (Takata et al., 2021). The fluxes of riverine dissolved  $^{137}Cs$  flowing into the lagoon and dissolved  $^{137}Cs$  through the desorption process were calculated using Eqs. (4),(5) and (6).

150  $FDC_{Sr} = DC_{Sr}Q_r$  , (4)

$FPC_{Sr} = PC_{Sr}Q_r$  , (5)

$FDC_{des} = 0.055FPC_{Sr}$  , (6)

where  $FDC_{Sr}$  is the flux of riverine dissolved  $^{137}Cs$  ( $Bq\ 12\ h^{-1}$ ),  $DC_{Sr}$  is the riverine  $^{137}Cs_{dis}$  ( $Bq\ m^{-3}$ ),  $Q_r$  is the volume of the river water discharge ( $m^3\ 12\ h^{-1}$ ),  $FPC_{Sr}$  is the flux of riverine particulate  $^{137}Cs$  ( $Bq\ 12\ h^{-1}$ ),  $PC_{Sr}$  is the riverine  $^{137}Cs_{par}$  ( $Bq\ m^{-3}$ ),  $FDC_{des}$  is the convert to  $^{137}Cs_{dis}$  from riverine  $^{137}Cs_{par}$  through the desorption process ( $Bq\ 12\ h^{-1}$ ). Additionally, fluxes of dissolved  $^{137}Cs$  supplying from the lagoon bottom were calculated using Eqs. (7). In this study, dissolved  $^{137}Cs$  in groundwater was not measured, so the flux of dissolved  $^{137}Cs$  from groundwater to the lagoon was not calculated.

155  $FDC_{Sbot} = FDC_{spot} - FDC_{Sr} - FDC_{des}$  , (7)

where  $FDC_{Sbot}$  is the flux of dissolved  $^{137}Cs$  supplying from the lagoon bottom ( $Bq\ 12h^{-1}$ ).

160 The fluxes of the dissolved  $^{137}Cs$  from the lagoon to the Pacific Ocean were estimated using Eq. (8), assuming that water volume outflowing to Pacific Ocean is the sum of the inflows of seawater, river water and SGD.

$FDC_{Sout} = DC_{Smean}(Q_s + Q_r + Q_{GW})$  , (8)

where  $FDC_{Sout}$  is the flux of the  $^{137}Cs_{dis}$  from the lagoon to the Pacific Ocean ( $Bq\ 12h^{-1}$ ),  $Q_{GW}$  is the volume of the SGD ( $m^3\ 12\ h^{-1}$ ).

165 Each flux was normalized to a time interval of 12 h to allow for the semidiurnal tidal periodicity in the lagoon (Kamo et al., 2014). Although the tidal prism does not fully represent the entire exchange of estuarine water with oceanic seawater entering from outside the lagoon, it is used here based on the simplified assumption that pure seawater flows in from the open ocean to help understand the monthly variation in the influx of dissolved  $^{137}Cs$  and the key factors maintaining relatively high  $^{137}Cs$  concentrations in the lagoon.

**3.1 <sup>137</sup>Cs Concentrations in River Waters**

Suspended particle concentrations, SPc ( $\text{g m}^{-3}$ ), particulate <sup>137</sup>Cs concentrations, <sup>137</sup>Cs<sub>par</sub> ( $\text{Bq m}^{-3}$ ), <sup>137</sup>Cs concentrations in suspended particles, <sup>137</sup>Cs<sub>sp</sub> ( $\text{Bq kg}^{-1}\text{-dry}$ ), dissolved <sup>137</sup>Cs concentrations, <sup>137</sup>Cs<sub>dis</sub> ( $\text{Bq m}^{-3}$ ), and apparent distribution coefficients,  $K_d$  ( $\text{L kg}^{-1}$ ) in the rivers flowing into the lagoon from 2021 to 2023 are shown in Figure 3. All riverine <sup>137</sup>Cs measurements and other parameters results and time series of <sup>137</sup>Cs<sub>par</sub> and <sup>137</sup>Cs<sub>dis</sub> are shown in Table S2 and Figure S1.

The mean SPc were 6.7, 7.3, 14.4, and 7.5  $\text{g m}^{-3}$  in Koizumi, Uda, Ume, and Nikkeshi Rivers, with respective median values of 2.5, 1.0, 15, and 5.4  $\text{g m}^{-3}$  (Figure 3a). The mean values are markedly higher than the median values because samples taken during increased rainfall in August 2022 increased the mean values. SPc in the Ume River were relatively high compared to those in the other three rivers; this was likely due to the reduced forest floor coverage in the Ume catchment (Table S1), which is known to engender increased soil erosion (Nishikiori et al., 2015). Similarly, the median <sup>137</sup>Cs<sub>par</sub> in the Koizumi, Uda, Ume, and Nikkeshi Rivers were 3.0, 2.0, 16, and 3.7  $\text{Bq m}^{-3}$ , respectively (Figure 3b). Increased SPc are related to increased <sup>137</sup>Cs<sub>par</sub> (Ueda et al., 2013), and both tend to increase during high flow conditions (Nagao et al., 2013; Niida et al., 2022). Therefore, the higher <sup>137</sup>Cs<sub>par</sub> in the Ume River was due to increased SPc in the river water. The mean <sup>137</sup>Cs<sub>sp</sub> in the Koizumi, Uda, Ume, and Nikkeshi Rivers were 1656, 1871, 2048, and 1224  $\text{Bq kg}^{-1}$ , respectively (Figure 3c). Although the mean inventory of deposited <sup>137</sup>Cs in the Uda catchment was 2–3 times higher than those in the other catchments, the mean <sup>137</sup>Cs<sub>sp</sub> in the Uda River was less than twice those in the other rivers. The mean <sup>137</sup>Cs<sub>dis</sub> in the Koizumi, Uda, Ume, and Nikkeshi Rivers were 2.2, 1.7, 2.6, and 3.5  $\text{Bq m}^{-3}$ , respectively (Figure 3d). The Uda River showed the lowest <sup>137</sup>Cs<sub>dis</sub> among the four rivers, similar to the distribution reported previously (Takata et al., 2022). Previous studies reported that <sup>137</sup>Cs<sub>dis</sub> in river water is higher in summer and lower in winter (Igarashi et al., 2022), but this study did not find a similar trend (Figure S1).

In catchments with high <sup>137</sup>Cs inventories, the <sup>137</sup>Cs<sub>sp</sub> and the <sup>137</sup>Cs<sub>dis</sub> flowing into the rivers tended to be high. We note, though, that the actual relationship is influenced by many factors such as topography, vegetation, rainfall patterns, and soil properties; accordingly, the relation between the <sup>137</sup>Cs concentration in the soils and <sup>137</sup>Cs in riverine particles or dissolved is not necessarily simply proportional. In downstream areas of catchments such as the Uda River, where soil <sup>137</sup>Cs concentrations are high in upstream areas and low in downstream areas, high <sup>137</sup>Cs<sub>sp</sub> and <sup>137</sup>Cs<sub>dis</sub> transported from the upstream area through the river may be diluted by downstream river waters containing less <sup>137</sup>Cs (Yamashiki et al., 2014).

$K_d$  values ranged from  $7.2 \times 10^4$  to  $3.7 \times 10^6$  L kg<sup>-1</sup> (Figure 3e), similar to those of rivers elsewhere in Fukushima Prefecture between 2011 and 2014, which ranged from  $7.7 \times 10^4$  to  $1.4 \times 10^6$  L kg<sup>-1</sup> (Taniguchi et al., 2019).

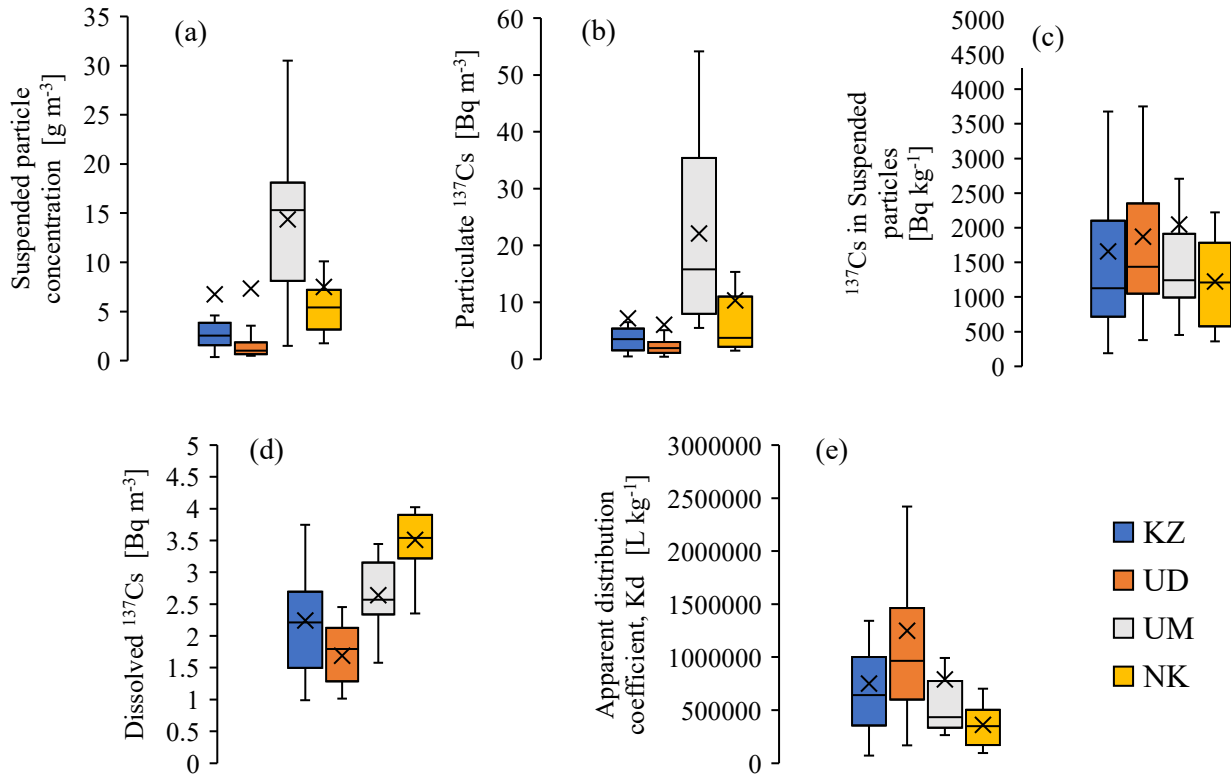


**Figure 3: Water conditions in the four in flowing rivers: (a) suspended particle concentration, (b) particulate <sup>137</sup>Cs concentration, (c) <sup>137</sup>Cs concentration in suspended particles, (d) dissolved <sup>137</sup>Cs concentration, and (e) the distribution coefficient ( $K_d$ ). Box plots represent the median and interquartile values, and the whiskers show the minimum and maximum values. Cross marks represent the arithmetic means of the results.**

## 3.2 <sup>137</sup>Cs Concentrations in Matsukawa-ura Lagoon

### 3.2.1 Changes in parameters due to salinity

The relationships between SPc, <sup>137</sup>Cs<sub>par</sub>, <sup>137</sup>Cs<sub>sp</sub>, <sup>137</sup>Cs<sub>dis</sub>,  $K_d$ , and salinity in rivers, within Matsukawa-ura lagoon, and in the nearshore area are shown in Figure 4. In addition, time series of <sup>137</sup>Cs<sub>par</sub> and <sup>137</sup>C<sub>dis</sub> are shown in Figure 5. The mean salinity in the lagoon during the study period was 29.1. All <sup>137</sup>Cs concentration and other parameters in the lagoon and coastal seawater (station URS) are listed in Table S3 and S4.

The mean and median SPc in the lagoon were 10.8 and 3.2 g m<sup>-3</sup>, respectively (range 0.3–208 g m<sup>-3</sup>). The mean and median <sup>137</sup>Cs<sub>par</sub> were 8.1 and 2.3 Bq m<sup>-3</sup>, respectively (range 0.1–123 Bq m<sup>-3</sup>). The mean and median <sup>137</sup>Cs<sub>sp</sub> were 1111 and 631 Bq kg<sup>-1</sup>

210 <sup>137</sup>Cs<sub>dis</sub>, respectively (range 100–16,434 Bq kg<sup>-1</sup>). The mean and median <sup>137</sup>Cs<sub>dis</sub> in the lagoon were 9.9 and 8.2 Bqm<sup>-3</sup>, respectively (range 2.5–31.3 Bq m<sup>-3</sup>). The *K<sub>d</sub>* values tended to decrease with increasing salinity (Figure 4e). Previous study has reported that SPc, <sup>137</sup>Cs<sub>par</sub> and <sup>137</sup>Cs<sub>sp</sub> tend to decrease with increasing salinity (Takata et al., 2022), which could be due to the dilution, coagulation, and settling of suspended particles along the salinity gradient as well as dilution by seawater with low <sup>137</sup>Cs concentrations, but our study did not find clear relationships (Figure 4a, b, c).

215 In contrast to <sup>137</sup>Cs<sub>par</sub> and <sup>137</sup>Cs<sub>sp</sub>, <sup>137</sup>Cs<sub>dis</sub> were higher in the lagoon than in the four inflowing rivers. <sup>137</sup>Cs<sub>dis</sub> also tended to increase with increasing salinity (Figure 4d), being the highest at salinities of 25–30, then decreasing at salinities above 30. This trend implies that the <sup>137</sup>Cs<sub>dis</sub> in the lagoon temporarily increases due to desorption of particulate <sup>137</sup>Cs from the rivers (Takata et al., 2020a) and the supply of dissolved <sup>137</sup>Cs from pore water in bottom sediments (Kambayashi et al., 2021; Takata et al., 2022) but is also diluted by the large amount of coastal seawater that flows into the lagoon. However, the large variation  
220 of <sup>137</sup>Cs<sub>dis</sub> at salinities of 25–30 (2.5–31.3 Bq m<sup>-3</sup>) may be due to seasonality and differences between sampling sites. The time series of <sup>137</sup>Cs<sub>dis</sub> and <sup>137</sup>Cs<sub>par</sub> at each sampling point in the lagoon area and nearshore area (Station URS) is shown in Figure 5. <sup>137</sup>Cs<sub>dis</sub> tended to decrease to the north and in proximity to the mouth of the lagoon, being highest at station UME, OSS and IWS on the south side of the lagoon (Figure 1b, Figure 5f–h, respectively). The tendency suggested that increasing mixing with coastal seawater containing low <sup>137</sup>Cs<sub>dis</sub> near the lagoon mouth such as station WKS, WKO and SKS (Figure 1b, Figure  
225 5b, c and e, respectively). It has been observed that some of radiocesium adsorbed to suspended particles flowing into the ocean is desorbed from the suspended particles due to competition with ionic species such as K<sup>+</sup> and NH<sub>4</sub><sup>+</sup> and converted to dissolved <sup>137</sup>Cs, resulting in a decrease in *K<sub>d</sub>* (Takata et al., 2020a; 2021), and similar trends were observed in our study. The <sup>137</sup>Cs<sub>dis</sub> at each station in the lagoon tended to be higher in summer and lower in winter, which was different from the trend in the rivers (Figure 5, S1). The next section discusses the seasonal variation of <sup>137</sup>Cs<sub>dis</sub> in the lagoon and its relationship with  
230 water temperature.

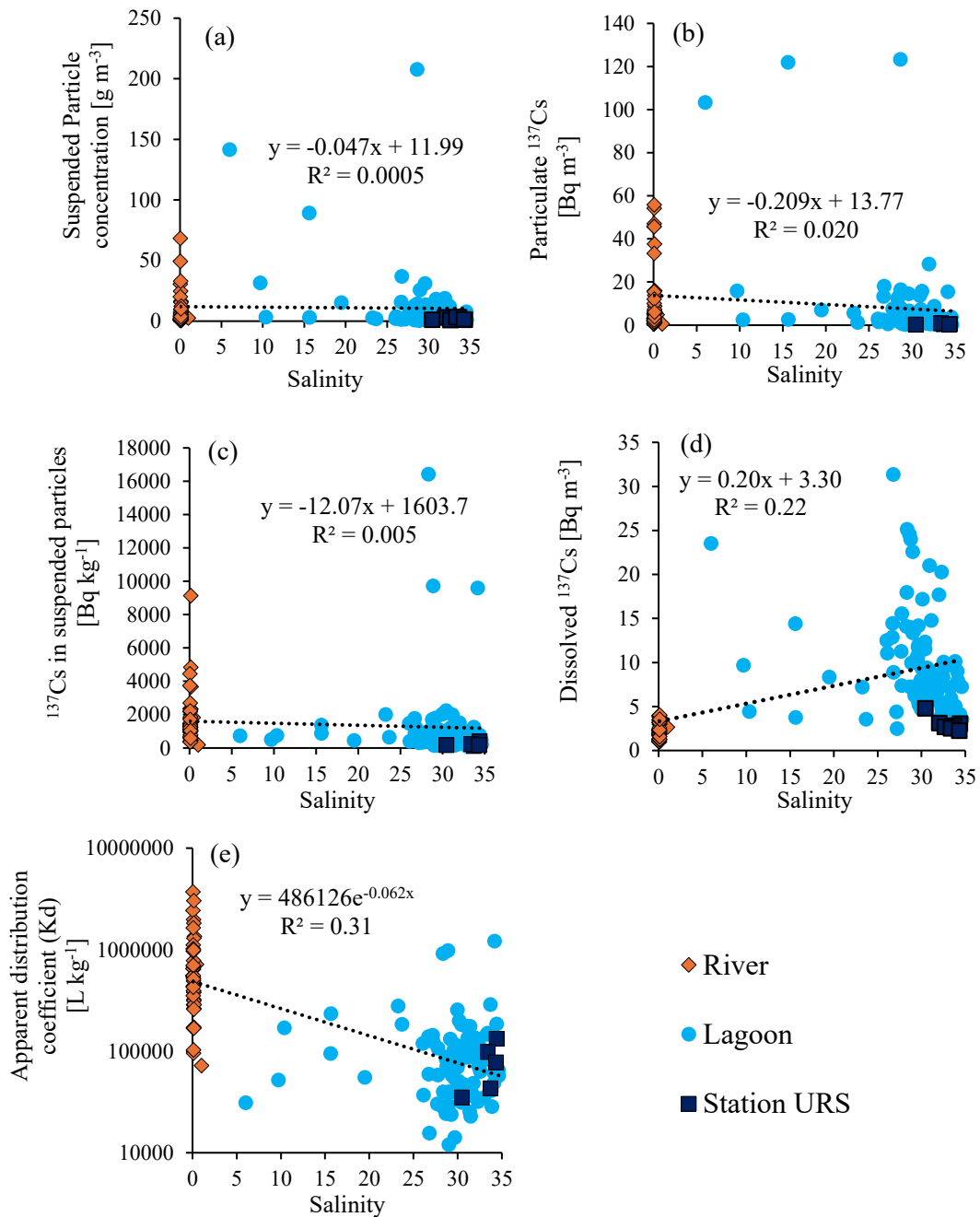


**Figure 4: Suspended particle concentration (a), particulate  $^{137}\text{Cs}$  concentration (b),  $^{137}\text{Cs}$  concentration in suspended particles (c), dissolved  $^{137}\text{Cs}$  concentration (d), and apparent distribution coefficient ( $K_d$ ) (e) plotted against salinity in Matsukawa-ura lagoon.**

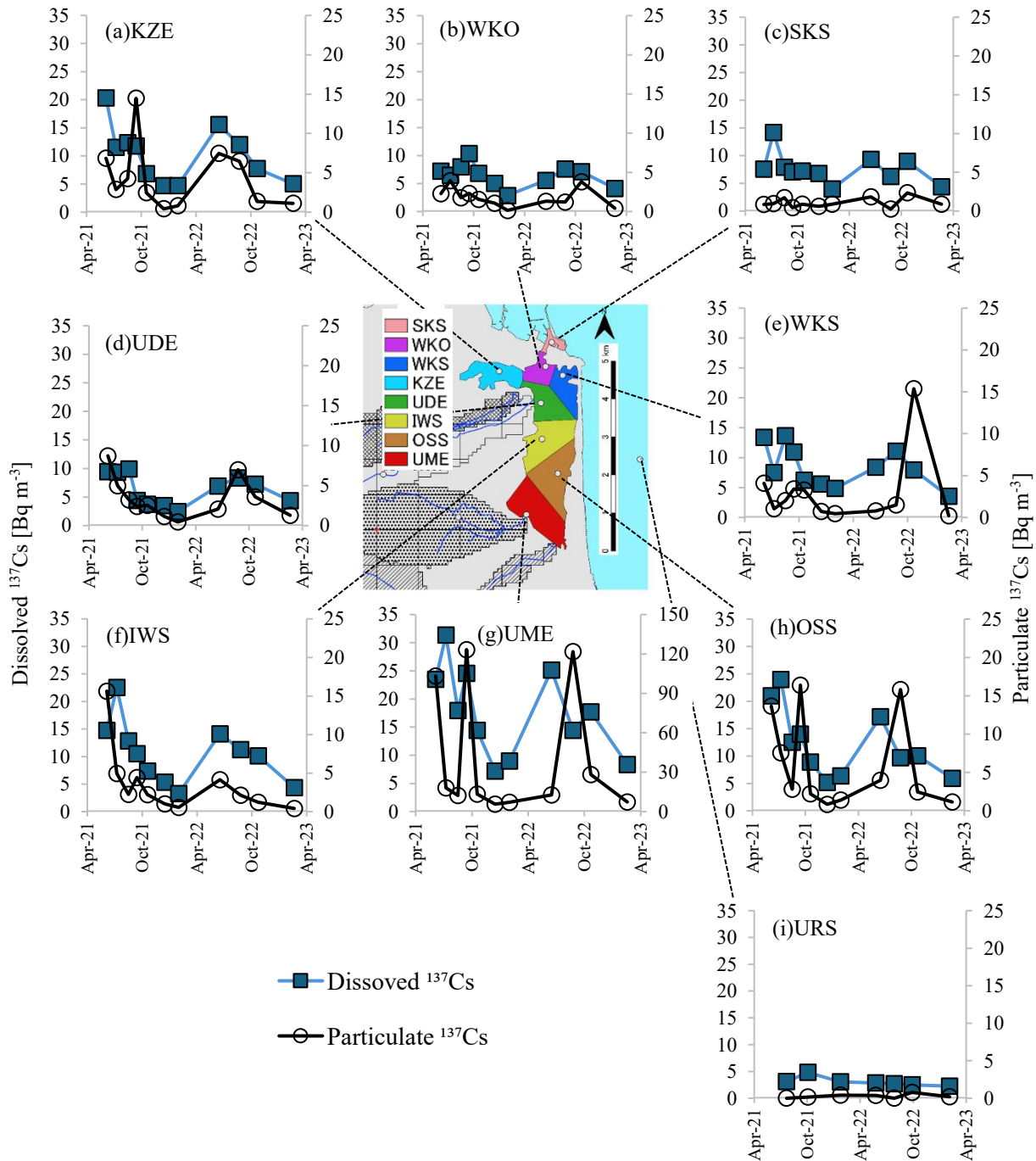


Figure 5: Time series of dissolved  $^{137}\text{Cs}$  and particulate  $^{137}\text{Cs}$  concentration in Matsukawa-ura lagoon.  $^{137}\text{Cs}$  concentrations were decay-corrected to the sampling date.

235

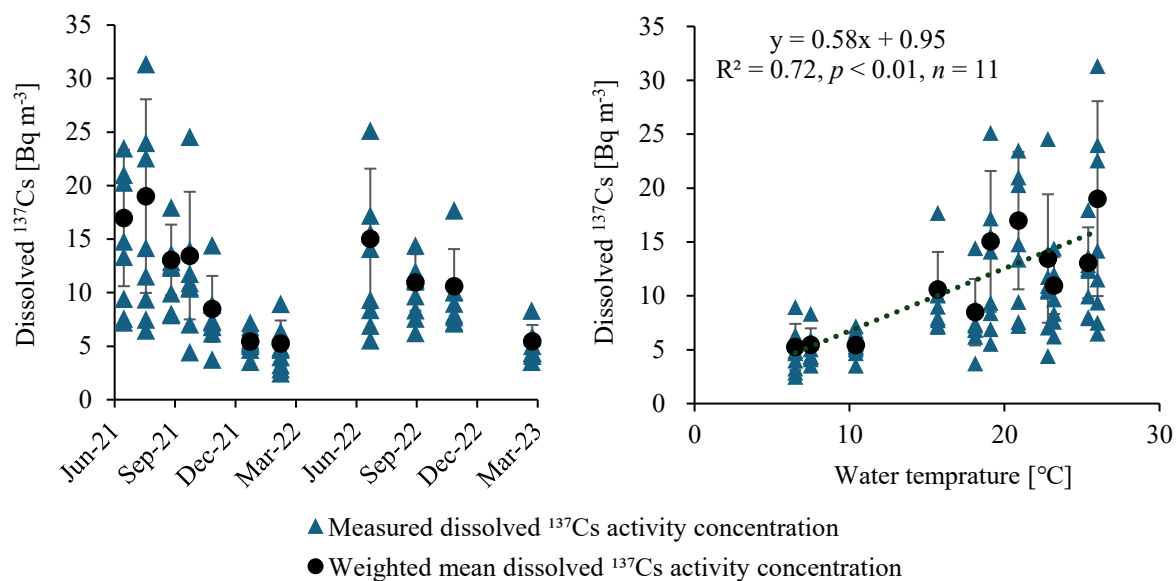
### 3.2.2 Seasonal Variation of dissolved $^{137}\text{Cs}$ in the lagoon

The time series of  $^{137}\text{Cs}_{\text{dis}}$  in the lagoon is shown in Figure 6a and relationship between  $^{137}\text{Cs}_{\text{dis}}$  and water temperature is shown in Figure 6b.

The weighted mean  $^{137}\text{Cs}_{\text{dis}}$  in the lagoon on each sampling date ranged from 5.3-19.0  $\text{Bq m}^{-3}$ , which was 2.4-8.6 times  
240 higher than the  $^{137}\text{Cs}_{\text{dis}}$  in coastal seawater, ranged from 2.2-4.8  $\text{Bq m}^{-3}$ , collected at station URS during the same period. The  
 $^{137}\text{Cs}_{\text{dis}}$  in the lagoon tended to be higher in the summer and lower in the winter (Figure 6a) and showed a significant correlation  
with water temperature (Figure 6b). The water depth of Matsukawa-ura lagoon is very shallow, averaging about 1m, and it has  
been indicated that about half of the water is exchanged during one tidal cycle (Kohata et al., 2003). For the simplicity in  
clarifying the seasonality of  $^{137}\text{Cs}_{\text{dis}}$  in the lagoon, we used the mean  $^{137}\text{Cs}_{\text{dis}}$  among several sampling stations which could  
245 represent the  $^{137}\text{Cs}_{\text{dis}}$  levels in the area of the lagoon. Actually, in February 2022 and 2023,  $^{137}\text{Cs}_{\text{dis}}$  ranged 2.5-9.0 and 3.5-8.3  
 $\text{Bq m}^{-3}$  with small variation, respectively, with weighted mean  $^{137}\text{Cs}_{\text{dis}}$  of 5.3 and 5.5  $\text{Bq m}^{-3}$ , but, weighted mean  $^{137}\text{Cs}_{\text{dis}}$  in  
June 2022 were 17.0 and 15.0  $\text{Bq m}^{-3}$ , respectively, about three times higher than winter season. These results suggest that  
seasonal variations are more influential than variations in concentrations between areas within the lagoon.

Previous studies revealed that water temperature influences the adsorption and desorption of  $^{137}\text{Cs}$  between solutions and  
250 particles with high affinities, such as clay minerals having “frayed-edge-sites” (FeS). Tertre et al. (2005) evaluated the  
effect of temperature on  $\text{Cs}^+$  behavior at low ionic strength under neutral conditions and reported that  $K_d$  decreases by a factor  
of 3 between 25 and 150 °C. Furthermore, Igarashi et al. (2022) reported a relationship between the  $K_d$  value of radiocesium  
and water temperature in the midstream catchment of the Abukuma River, which flows through Fukushima Prefecture; they  
suggested that  $K_d$  decreases as water temperature increases. Furthermore, Nagao et al. (2020) reported that 0.1% of  $^{137}\text{Cs}$  were  
255 desorbed from sand samples in ultrapure water; 3.7% in a 25% seawater solution; 7.1% in a 50% seawater solution; and 10%–  
12% in 100% seawater, in artificial seawater, and in a 470 mM NaCl + 8 mM KCl solution. In other words, it is possible that  
the desorption of  $^{137}\text{Cs}$  is largely completed at the salinity of a 50% seawater solution. In Matsukawa-ura lagoon (average  
salinity is 29.1), where the study was conducted, the desorption of  $^{137}\text{Cs}$  by ion exchange in seawater was largely complete,  
implying that the effect of water temperature dominates over that of salinity in the adsorption and desorption process of  $^{137}\text{Cs}$   
260 in seawater.

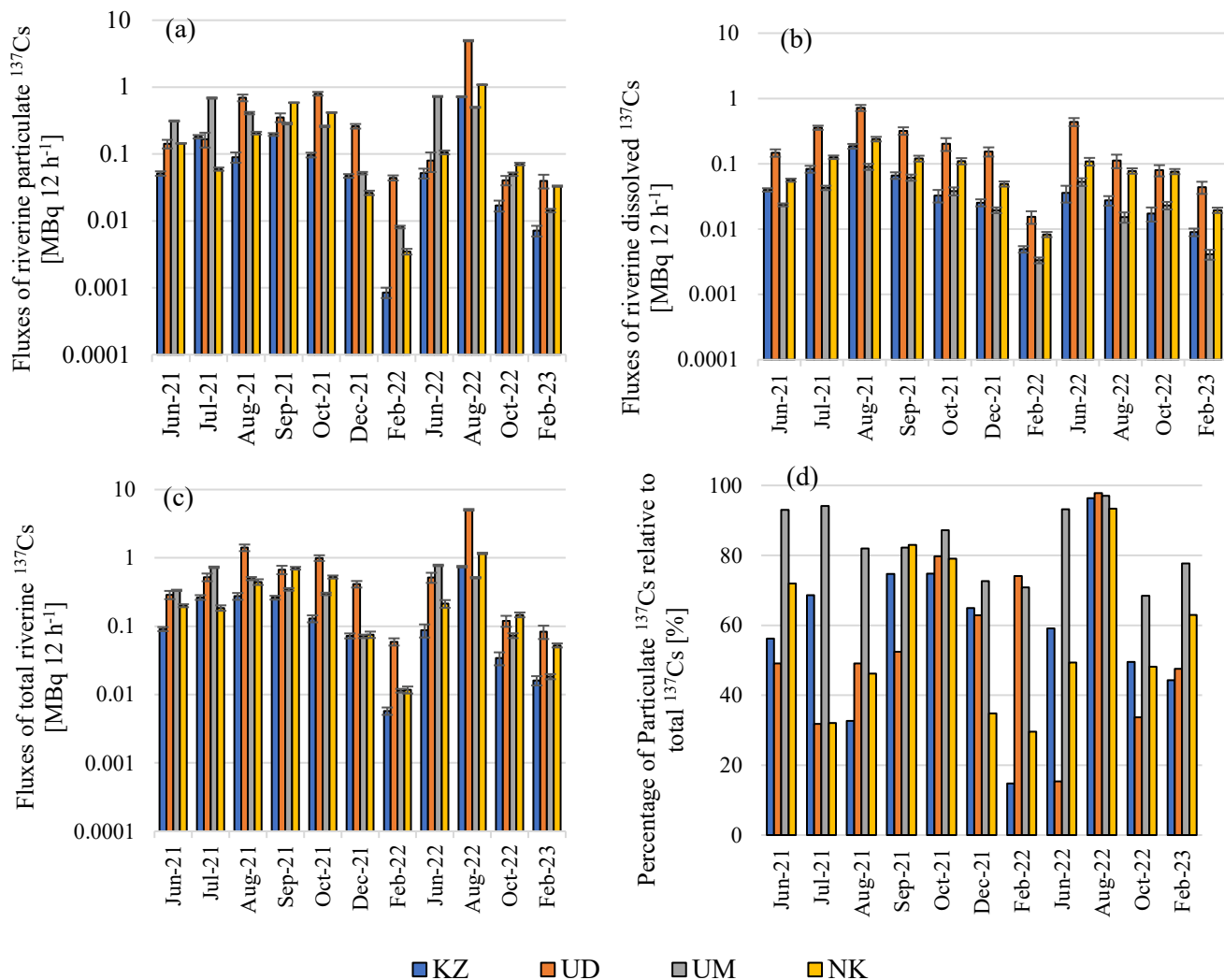
In the next section, we use mass balance calculations to analyze the sources of dissolved  $^{137}\text{Cs}$  in the lagoon and compare  
the contributions of river inputs against the supply from bottom sediments.



265 **Figure 6: Time series of dissolved  $^{137}\text{Cs}$  concentrations (a) and dissolved  $^{137}\text{Cs}$  concentrations versus water temperature (b) in Matsukawa-ura lagoon from June 2021 to February 2023. Black bars represent the standard deviation of the dissolved  $^{137}\text{Cs}$  concentrations on each sampling date.**

### 3.3 Mass Balance Calculations

270 The fluxes of  $^{137}\text{Cs}$  from each river into the lagoon are shown in Fig 7. The mean fluxes of particulate  $^{137}\text{Cs}$  from each river to the lagoon during the sampling campaign were 0.13, 0.69, 0.30 and 0.25 MBq  $12\text{ h}^{-1}$  for Koizumi, Uda, Ume and Nikkeshi River, respectively. The mean fluxes of dissolved  $^{137}\text{Cs}$  from each river were 0.048, 0.24, 0.034 and 0.090 MBq  $12\text{ h}^{-1}$  for Koizumi, Uda, Ume and Nikkeshi River, respectively. The fluxes of sum of  $^{137}\text{Cs}_{\text{par}}$  and  $^{137}\text{Cs}_{\text{dis}}$  from Uda River, which had lower  $^{137}\text{Cs}_{\text{par}}$  and  $^{137}\text{Cs}_{\text{dis}}$  than the other three rivers (Figure 3(b), (d)), were predominant (Figure 7c). This is because the water discharge of Uda River is several times higher than that of the other three rivers (Table S1). The mean proportion of particulate  $^{137}\text{Cs}$  in the total flux was about 50%–60% in all except Ume River. However, during high flow conditions, August 2022, particulate  $^{137}\text{Cs}$  accounted for more than 90% of the total flux in all rivers (Figure 7d), as reported in previous studies (Nagao et al., 2013; Yamashiki et al., 2014; Niida et al., 2022). The flux of  $^{137}\text{Cs}$  flowing into the lagoon from the four rivers at 12-h intervals ranged from 0.06 to 7.24 MBq  $12\text{ h}^{-1}$ , the total dissolved  $^{137}\text{Cs}$  flux from 0.03 to 1.23 MBq  $12\text{ h}^{-1}$ . In addition, assuming that 5.5% of riverine particulate  $^{137}\text{Cs}$  is desorbed to dissolved  $^{137}\text{Cs}$  through the desorption process after inflow the lagoon (Takata et al., 2021), it was estimated that 0.003 to 0.40 MBq  $12\text{ h}^{-1}$  was desorbed to dissolved  $^{137}\text{Cs}$  from particulate  $^{137}\text{Cs}$ .



280 **Figure 7: Fluxes of riverine particulate  $^{137}\text{Cs}$  (a), dissolved  $^{137}\text{Cs}$  (b) and total  $^{137}\text{Cs}$  (c) in each river. Proportion of particulate  $^{137}\text{Cs}$  flux in the total  $^{137}\text{Cs}$  flux (d). Black bars represent the measurement error of  $^{137}\text{Cs}$ .**

The potential fluxes of dissolved  $^{137}\text{Cs}$  supplying to the lagoon and flux of dissolved  $^{137}\text{Cs}$  that flowed out from the lagoon into the Pacific Ocean are shown in Figure 8a. Fluxes of dissolved  $^{137}\text{Cs}$  supplied to the lagoon from the rivers, desorbed from riverine particles and supplied from the lagoon bottom are shown in Figure 8b. Details of the calculation results are shown in  
 285 Table S5. The mean water depth at the station WKO, located at mouth of the lagoon, was 1.9 m, with a maximum of 2.2 m and a minimum of 1.7 m, and the difference between the maximum values was about 50 cm (Figure S2). Therefore, the exchange volume in the lagoon was assumed to be constant throughout the year, making it possible to compare between seasons. The weighted mean  $^{137}\text{Cs}_{\text{dis}}$  in the lagoon during the study period was 5.3–19.0 Bq m<sup>-3</sup>, whereas the  $^{137}\text{Cs}_{\text{dis}}$  in

nearshore seawater outside the lagoon (station URS) during the same period was 2.2–4.8 Bq m<sup>-3</sup>. This result indicates that  
290 mixing in river mouths in the lagoon increased the <sup>137</sup>Cs<sub>dis</sub> by 0.5–16.8 Bq m<sup>-3</sup> after seawater flowed into the lagoon. Therefore,  
3.4–121 MBq 12 h<sup>-1</sup> of dissolved <sup>137</sup>Cs was added to the lagoon (Figure 8a). However, while the fluxes of dissolved and  
desorbed <sup>137</sup>Cs from the river were 0.03–1.23 MBq 12 h<sup>-1</sup> and 0.003–0.40 MBq 12 h<sup>-1</sup>, respectively. The fluxes dissolved <sup>137</sup>Cs  
supplied from the lagoon bottom were 4.8–120 MBq 12 h<sup>-1</sup>, which were much greater than the fluxes of <sup>137</sup>Cs from the rivers.  
It has been reported that the <sup>137</sup>Cs<sub>dis</sub> in groundwater collected in the lagoon catchment in 2015–2016 were below 9.7 Bq m<sup>-3</sup>  
295 (Kambayashi et al., 2021). Therefore, the supply of <sup>137</sup>Cs dissolved from bottom sediments must be much greater than that  
from rivers. Kambayashi et al. (2021) measured the <sup>137</sup>Cs concentration in pore water in sediments of Matsukawa-ura lagoon  
in 2016 and estimated the flux from the sediments to be 139–293 MBq day<sup>-1</sup>, suggesting that the supply of <sup>137</sup>Cs from bottom  
sediments may account for more than 90% of the supply of <sup>137</sup>Cs to Matsukawa-ura lagoon, which is generally consistent with  
our estimates. These results suggest that the amount of <sup>137</sup>Cs deposited in marine sediments in the early stages of the accident  
300 and dissolved and dispersed into the seawater may not change significantly, whether three or ten years have passed since the  
accident. Thus, as more time passes since the accident and the supply of <sup>137</sup>Cs to coastal waters from rivers decreases due to  
the decommissioning of contaminated soils in their catchment areas, the contribution of the dissolution of this nuclide from  
bottom sediments may become relatively greater.

Based on our results, we conclude that <sup>137</sup>Cs in bottom sediments, deposited during the early stages of FDNPP accident,  
305 gradually dissolves when pore waters are exposed to seawater flowing into the lagoon. However, warmer seawater  
temperatures during the summer may further accelerate the dissolution process. This finding implies that the processes  
observed in the lagoon have changed the spatiotemporal distribution of <sup>137</sup>Cs in the coastal waters of Fukushima Prefecture.

In this study, the fluxes of dissolved <sup>137</sup>Cs flowing from the lagoon to the Pacific Ocean were estimated to be 38 to 142 MBq  
12 h<sup>-1</sup>. Niida et al. (2022) estimated the fluxes of <sup>137</sup>Cs flowing to the Pacific Ocean during July 27–29, 2020, when the total  
310 rainfall was about 80mm, were 107, 120 and 109 MBq in the Niida, Ukedo and Takase River catchment. These rivers and their  
catchments are located closer to FDNPP than Matsukawa-ura and have a much higher <sup>137</sup>Cs inventories. The mean <sup>137</sup>Cs  
inventories in each catchment were 853, 2359, 701 kBq m<sup>-2</sup> for Niida, Ukedo and Takase River, respectively. However, this  
is comparable to the flux of dissolved <sup>137</sup>Cs we estimated flowing from Matsukawa-ura into the Pacific Ocean in half a day.  
Therefore, these results suggest that the impact of dissolved <sup>137</sup>Cs outflow from Matsukawa-ura into the coastal waters of  
315 Fukushima Prefecture is relatively greater than that of other rivers in Fukushima Prefecture.

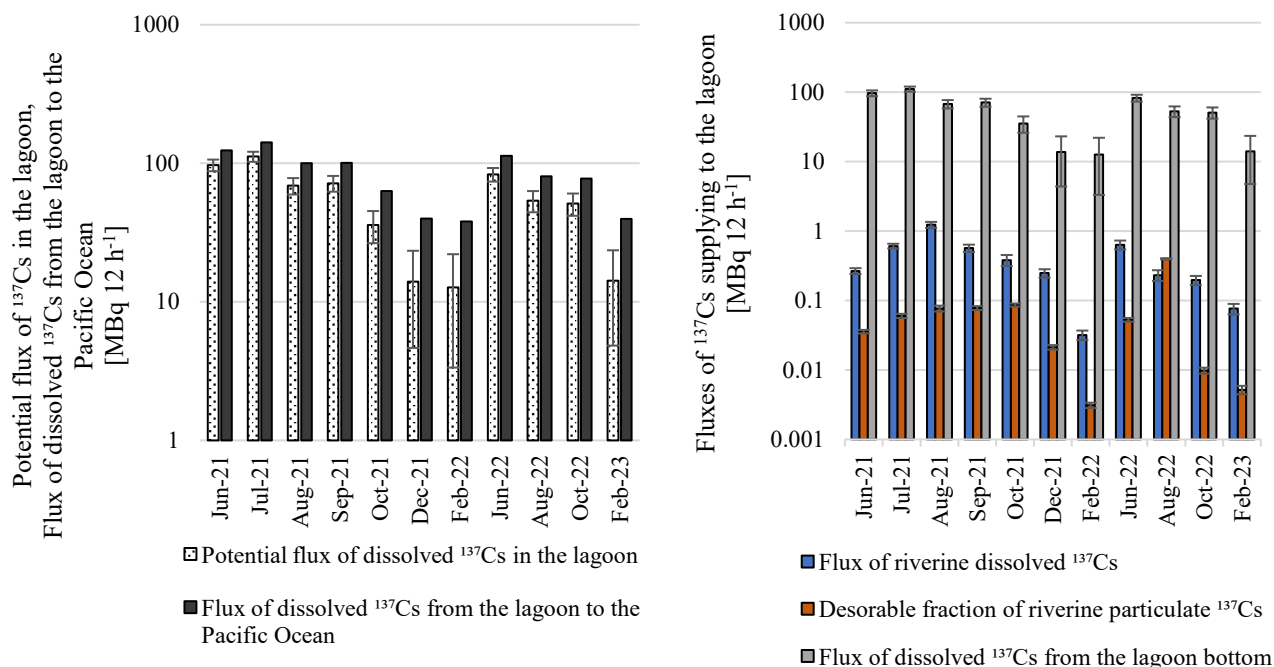


**Figure 8: Potential fluxes of dissolved  $^{137}\text{Cs}$  supplied to Matsukawa-ura lagoon and fluxes of dissolved  $^{137}\text{Cs}$  from the lagoon to the Pacific Ocean (a). Fluxes of dissolved  $^{137}\text{Cs}$  supplied to the lagoon from the rivers, desorbed from riverine particles and the lagoon bottom in the lagoon (b). Black bars represent the measurement error of  $^{137}\text{Cs}$ .**

#### 4 Conclusion

320 We investigated the spatial and seasonal dynamics of  $^{137}\text{Cs}$  in Matsukawa-ura lagoon, a semi-closed estuarine area approximately 40 km north of the Fukushima Daiichi Nuclear Power Plant, Japan. The dissolved  $^{137}\text{Cs}$  concentrations in the lagoon were higher than that in the river water flowing into the lagoon and in the coastal seawater, suggesting the influence of desorption from suspended sediments due to increasing salinity. Furthermore, it was found that dissolved  $^{137}\text{Cs}$  concentrations in the lagoon were high in summer and low in winter, suggesting influence of water temperatures.

325 Quantification of the sources by mass balance calculations revealed that the supply of dissolved  $^{137}\text{Cs}$  from bottom sediments was much greater than the supply of dissolved  $^{137}\text{Cs}$  from rivers and suspended sediments. These results suggest that continuous  $^{137}\text{Cs}$  input from rivers are unlikely to have a strong impact on the spatiotemporal variation of dissolved  $^{137}\text{Cs}$  concentrations in the lagoon, and we conclude that  $^{137}\text{Cs}$  in the sediments deposited during the early stages of Fukushima Daiichi Nuclear Power Plant accident was exposed to seawater flowing into the lagoon and gradually dissolved. In addition, higher seawater  
 330 temperatures in summer may accelerate the dissolution of  $^{137}\text{Cs}$  from bottom sediments. Furthermore, flux of dissolved  $^{137}\text{Cs}$  flowing from Matsukawa-ura lagoon into Pacific Ocean in half day is comparable to the flux of dissolved  $^{137}\text{Cs}$  flowing from other rivers in Fukushima prefecture to the Pacific Ocean in about one day under high flow conditions. These results suggest

that to understand why the dissolved  $^{137}\text{Cs}$  is high in coastal areas of Fukushima Prefecture, it is necessary to strengthen monitoring of bottom sediments and pore water, particularly in river mouths and coastal areas, to clarify the dynamics and impact of  $^{137}\text{Cs}$  desorbed from bottom sediments. Future research should investigate the relationship between  $^{137}\text{Cs}$  concentration in the bottom sediments and pore water of estuaries and coastal areas, and not only water quality but also seasonal variations in water temperature.

### Team list

#### Corresponding Author

340 Takuya Niida – *Graduate School of Symbiotic Systems Science and Technology, Fukushima University, 1 Kanayagawa, Fukushima City, Fukushima 960-1296, Japan; Email (present): s2571005@ipc.fukushima-u.ac.jp*

*Laboratory for Instrumentation and Analysis, Environmental Engineering Division, KANSO TECHNOS CO., LTD, 3-1-1, Higashikuraji, Katano City, Osaka 576-0061, Japan; Phone: +81-72-810-6551; Email (permanent): niida\_takuya@kanso.co.jp*

345 Authors

Hyoe Takata - *Institute of Environmental Radioactivity, Fukushima University, 1 Kanayagawa, Fukushima City, Fukushima 960-1296, Japan; Email: h.takata@ier.fukushima-u.ac.jp*

Sho Watanabe - *Fukushima Prefectural Research Institute of Fisheries Resources, 1-1-14 Koyo, Soma City, Fukushima 970-0005, Japan; Email: watanabe\_shou\_01@pref.fukushima.lg.jp*

350 Shinya Namura - *Laboratory for Instrumentation and Analysis, Environmental Engineering Division, KANSO TECHNOS CO., LTD, 3-1-1, Higashikuraji, Katano City, Osaka 576-0061, Japan; Email: namura\_shinya@kanso.co.jp*

Toshihiro Wada - *Institute of Environmental Radioactivity, Fukushima University, 1 Kanayagawa, Fukushima City, Fukushima 960-1296, Japan; Email: t-wada@ipc.fukushima-u.ac.jp*

### Author contribution

355 The manuscript was written through contributions of all authors. All authors have given approval to the final version of the manuscript.

### Competing interest

The authors declare that they have no conflict of interest.

## Acknowledgements

360 We are grateful to researchers of the Fukushima Prefectural Research Institute of Fisheries Resources for their cooperation during sampling.

## Financial support

This research is an achievement of " Stabilizing resources through effective release of seedlings using ICT infrastructure" (JPFR23060109, JPFR24060109, JPFR25060109) among advanced technology development projects in the field of  
365 agriculture, forestry and fisheries. (Fukushima Institute for Research, Education and Innovation (F-REI)).

## References

- Aoyama, M.; Uematsu, M.; Tsumune, M.; Hamajima, Y.: Surface pathway of radioactive plume of TEPCO Fukushima NPP1 released  $^{134}\text{Cs}$  and  $^{137}\text{Cs}$ . *Biogeosciences.*, 10, 3067-3078. <https://doi.org/10.5194/bg-10-3067-2013>, 2013.
- Aoyama, M.; Kajino, M.; Tanaka, T.Y.; Sekiyama, T.T.; Tsumune, D.; Tsubono, T.; Hamajima, Y.; Inomata, Y.; Gamo, T. :  $^{134}\text{Cs}$  and  $^{137}\text{Cs}$  in the North Pacific Ocean derived from the TEPCO Fukushima Dai-ichi Nuclear Power Plant accident, Japan in March 2011. Part Two: estimation of  $^{134}\text{Cs}$  and  $^{137}\text{Cs}$  inventories in the North Pacific Ocean. *J. Oceanogr.*, 72, 67-76. <https://doi.org/10.1007/s10872-015-0332-2>, 2016.
- Arita, K.; Yabe, T.; Hayashi, S.: Actual situation of concentration and inventory of radioactive cesium in Matsukawa-ura Lagoon sediment, Fukushima Prefecture. *J. Jpn. Soc. Civ. Eng. Ser. G (Environ. Res.)*, 70, III\_225–III\_231 (in Japanese with English abstract). [https://doi.org/10.2208/jscejer.70.III\\_225](https://doi.org/10.2208/jscejer.70.III_225), 2014.
- Fukushima prefecture Website; <https://www.pref.fukushima.lg.jp/sec/37380b/suion.html>. (Accessed 30 June 2024).
- IAEA, 2004. Sediment Distribution Coefficients and Concentration Factors for Biota in the Marine Environment. Technical Reports Series No. 422.
- Igarashi, Y.; Nanba, K.; Wada, T.; Wakiyama, Y.; Onda, Y.; Moritaka, S.; Konoplev, A.: Factors controlling the dissolved  $^{137}\text{Cs}$  seasonal fluctuations in the Abukuma river under the influence of the Fukushima nuclear power plant accident. *J. Geophys. Res.: Biogeosci.*, 127 (1), e2021JG006591. <https://doi.org/10.1029/2021JG006591>, 2022.
- Japan Atomic Energy Agency Web site; Results of the Fourth Airborne Monitoring Survey by MEXT. [https://emdb.jaea.go.jp/emdb\\_old/portals/b1020201/](https://emdb.jaea.go.jp/emdb_old/portals/b1020201/). (Accessed 15 April 2024).

- Kambayashi, S.; Zhang, J.; Narita, H.: Significance of Fukushima-derived radiocaesium flux via river-estuary-ocean system. Sci. Total Environ., 793, 148456. <https://doi.org/10.1016/j.scitotenv.2021.148456>, 2021.
- 385
- Kamo, T.; Suzuki, M.; Wada, T.; Iwasaki, T.; Watanabe, T.; Nishi, R.; Tsurunari, Y.: Estimation of freshwater discharge and field observation on aquatic environment around the entrance of Matsukawaura inlet. J. Jpn. Soc. Civ. Eng. Ser. B3 Ocean. Eng., 70, I\_1020–I\_1025 (in Japanese with English abstract). [https://doi.org/10.2208/jscejoe.70.I\\_1020](https://doi.org/10.2208/jscejoe.70.I_1020), 2014.
- Kohata, K.; Hiwatari, T.; Hagiwara, T. Natural water-purification system observed in a shallow coastal lagoon: Matsukawaura, Japan. Mar. Pollut. Bull., 47, 148-154. [https://doi.org/10.1016/S0025-326X\(03\)00055-9](https://doi.org/10.1016/S0025-326X(03)00055-9), 2003.
- 390
- Kusakabe, M.; Takata, H.: Temporal trends of <sup>137</sup>Cs concentration in seawaters and bottom sediments in coastal waters around Japan: implications for the Kd concept in the dynamic marine environment. J. Radioanal. Nucl. Chem., 323, 567–580. <https://doi.org/10.1007/s10967-019-06958-z>, 2020.
- Li, Y.-H.; Burkhardt, L.; Teraoka, H.: Desorption and coagulation of trace elements during estuarine mixing. Geochim. Cosmochim. Acta., 48, 1879–1884. [https://doi.org/10.1016/0016-7037\(84\)90371-5](https://doi.org/10.1016/0016-7037(84)90371-5), 1984.
- 395
- Machida, M.; Yamada, S.; Iwata, A.; Otsuka, S.; Kobayashi, T.; Watanabe, M.; Funasaka, H.; Morita, T.: Seven-year temporal variation of Cesium-137 discharge inventory from the port of Fukushima Dai-ichi Nuclear Power Plant. Trans. At. Energy Soc. Japan., 18, 226–236 (in Japanese with English abstract). <https://doi.org/10.3327/taesj.J18.030>, 2019.
- Nagao, S.; Kanamori, M.; Ochiai, S.; Tomihara, S.; Fukushi, K.; Yamamoto, M.: Export of <sup>134</sup>Cs and <sup>137</sup>Cs in the Fukushima river systems at heavy rains by Typhoon Roke in September 2011. Biogeosci. Discuss., 10, 6212-6223. <https://doi.org/10.5194/bg-10-6215-2013>, 2013.
- 400
- Nagao, S.; Terasaki, S.; Ochiai, S.; Fukushi, K.; Tomihara, S.; Charette, M. A.; Buesseler, K. O.: Desorption Behavior of Fukushima-derived Radiocesium in Sand Collected from Yotsukura Beach in Fukushima Prefecture. Anal. Sci., 36, 569-573. <https://doi.org/10.2116/analsci.19SBP08>, 2020.
- 405
- Niida, T.; Wakiyama, Y.; Takata, H.; Taniguchi, K.; Kurosawa, H.; Fujita, K.; Konoplev, A.: A comparative study of riverine <sup>137</sup>Cs dynamics during highflow events at three contaminated river catchments in Fukushima. Sci. Total Environ., 821, 153408. <https://doi.org/10.1016/j.scitotenv.2022.153408>, 2022.
- Nishikiori, T.; Ito, S.; Tsuji, H.; Yasutaka, T.; Hayashi, S.: Influence of Forest Floor Covering on Radiocesium Wash-off Associated with Forest Soil Erosion. J. Jpn. For. Soc., 97, 63–69 (in Japanese with English abstract).
- 410
- <https://doi.org/10.4005/jjfs.97.63>, 2015.

- Noda, T.; Wada, T.; Mitamura, H.; Kume, M.; Komaki, T.; Fujita, T.; Sato, T.; Narita, K.; Yamada, M.; Matsumoto, A.; Hori, T.; Takagi, J.; Kutzer, A.; Arai, N.; Yamashita, Y.: Migration, residency and habitat utilisation by wild and cultured Japanese eels (*Anguilla japonica*) in a shallow brackish lagoon and inflowing rivers using acoustic telemetry. *J. Fish Biol.*, 98, 507–525. <https://doi.org/10.1111/jfb.14595>, 2021.
- 415 Otsuka, S.; Kambayashi, S.; Fukuda, M.; Tsuruta, T.; Misonou, T.; Suzuki, T.; Aono, T.: Behavior of radiocesium in sediments in Fukushima coastal waters: verification of desorption potential through pore water. *Environ. Sci. Technol.*, 54, 13778–13785. <https://doi.org/10.1021/acs.est.0c05450>, 2020.
- Sanial, V.; Buessler, K.O.; Charette, M.A.; Nagao, S.: Unexpected source of Fukushima-derived radiocesium to the coastal ocean of Japan. *PNAS.*, 114(42), 11092–11096. <https://doi.org/10.1073/pnas.1708659114>, 2017.
- 420 Suzuki, S.; Amano, Y.; Enomoto, M.; Matsumoto, A.; Morioka, Y.; Sakuma, K.; Tsuruta, T.; Kaeriyama, H.; Miura, H.; Tsumune, D.; Kamiyama, K.; Wada, T.; Takata, H.: Temporal variability of  $^{137}\text{Cs}$  concentrations in coastal sediments off Fukushima. *Sci. Total Environ.*, 831, 154670. <https://doi.org/10.1016/j.scitotenv.2022.154670>, 2022.
- Takata, H.; Aono, T.; Aoyama, M.; Inoue, M.; Kaeriyama, H.; Suzuki, S.; Tsuruta, T.; Wada, T.; Wakiyama, Y.: Suspended particle–water interactions increase dissolved  $^{137}\text{Cs}$  activities in the nearshore seawater during typhoon Hagibis. *Environ. Sci. Technol.*, 54, 10678–10687. <https://doi.org/10.1021/acs.est.0c03254>, 2020a.
- 425 Takata, H.; Inatomi, N.; Kudo, N.: The contribution of  $^{137}\text{Cs}$  export flux from the Tone River Japan to the marine environment. *Sci. Total Environ.*, 701, 134550. <https://doi.org/10.1016/j.scitotenv.2019.134550>, 2020b.
- Takata, H.; Wakiyama, Y.; Niida, T.; Igarashi, Y.; Konoplev, A.; Inatomi, N.: Importance of desorption process from Abukuma River’s suspended particles in increasing dissolved  $^{137}\text{Cs}$  in coastal water during river-flood caused by typhoons. *Chemosphere.*, 281, 130751. <https://doi.org/10.1016/j.chemosphere.2021.130751>, 2021.
- 430 Takata, H.; Wada, T.; Aono, T.; Inoue, M.; Kanasashi, T.; Suzuki, S.; Amano, Y.: Factors controlling dissolved  $^{137}\text{Cs}$  activities in coastal waters on the eastern and western sides of Honshu, Japan, *Environ. Sci. Total Environ.*, 806, 151216. <https://doi.org/10.1016/j.scitotenv.2021.151216>, 2022.
- Taniguchi, K.; Onda, Y.; Smith, H.G.; Blake, W.; Yoshimura, K.; Yamashiki, Y.; Kuramoto, T.; Saito, K.: Transport and redistribution of radiocaesium in Fukushima fallout through rivers. *Environ. Sci. Technol.*, 53, 12339–12347. <https://doi.org/10.1021/acs.est.9b02890>, 2019.

- Tertre, E.; Berger, G.; Castet, S.; Loubet, M.; Giffaut, E.: Experimental sorption of  $\text{Ni}_2^+$ ,  $\text{Cs}^+$  and  $\text{Ln}_3^+$  onto a montmorillonite up to 150°C. *Geochim. Cosmochim. Acta.*, 69(21), 4937–4948. <https://doi.org/10.1016/j.gca.2005.04.024>, 2005.
- 440 Tsuji, H.; Nishikiori, T.; Ito, S.; Ozaki, H.; Watanabe, M.; Sakai, M.; Ishii, Y.; Hayashi, S.: Influential factors of long-term and seasonal  $^{137}\text{Cs}$  change in agricultural and forested rivers: Temperature, water quality and an intense Typhoon Event. *Environ. Pollut.*, 338, 122617. <https://doi.org/10.1016/j.envpol.2023.122617>, 2023.
- Turner, A.: Trace-metal partitioning in estuaries: importance of salinity and particle concentration. *Mar. Chem.*, 54, 27–39. [https://doi.org/10.1016/0304-4203\(96\)00025-4](https://doi.org/10.1016/0304-4203(96)00025-4), 1996.
- 445 Ueda, S.; Hasegawa, H.; Kakiuchi, H.; Akata, N.; Ohtsuka, Y.: Fluvial discharges of radiocaesium from watersheds contaminated by the Fukushima Dai-ichi Nuclear Power Plant accident, Japan. *J. Environ. Radioact.*, 118, 96-104. <https://doi.org/10.1016/j.jenvrad.2012.11.009>, 2013.
- Wada, T.; Kamiyama, K.; Shimamura, S.; Matsumoto, I.; Mizuno, T.; Nemoto, Y.: Habitat utilization, feeding, and growth of wild spotted halibut *Verasper variegatus* in a shallow brackish lagoon: Matsukawa-ura, northeastern Japan. *Fish. Sci.*, 77, 785–793. <https://doi.org/10.1007/s12562-011-0385-0>, 2011.
- 450 Yamashiki, Y.; Onda, Y.; Smith, H.G.; Blake, W.H.; Wakahara, T.; Igarashi, Y.; Matsuura, Y.; Yoshimura, K.: Initial flux of sediment-associated radiocesium to the ocean from the largest river impacted by Fukushima Daiichi Nuclear Power Plant. *Sci. Rep.*, 4, 3714. <https://doi.org/10.1038/srep03714>, 2014.